AD-A110 180 HAWAII UNIV HONOLULU F/G 20/6

LONG BASELINE MEASUREMENTS OF LIGHT TRANSMISSION.(U)

DEC 81 H BRADNER, G BLACKINTON N00014-79-C-0818

UNCLASSIFIED NL

END

DATE FILMED

2 82

DTIC

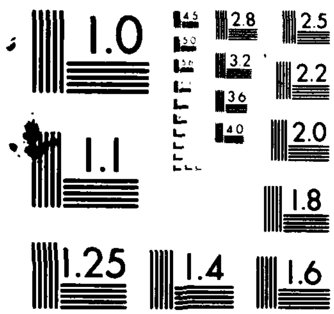

MICROCOPY RESOLUTION TEST CHART
NATIONAL BUREAU OF STANDARDS 1963 A

AD A110180

LONG BASELINE MEASUREMENTS OF LIGHT TRANSMISSION

Hugh Bradner* and Grant Blackinton
University of Hawaii
Honolulu, HI 96822 USA

Dec. 1981

ABSTRACT

Measurements have been made of the uncollimated ("poor geometry") 1/e transmission distance of light in seawater, at approximately 1 km and 1.5 km depths, 27 km east of the center of the proposed DUMAND site off Keahole Point, Hawaii. The measurements were made with 480 nanometer blue-breen light, through path lengths of 84.0 meters and 7.86 meters.

Contract N00014-79-C-0818

Introduction

Measurements of attenuation length of light in seawater usually have been made with a rigid instrument having a well collimated light path about 1 meter long. Both scattering and absorption reduce the light flux that reaches the detector. Such highly collimated measurements are important for establishing the fundamental optical properties of the sea water, and for characterizing its image-forming characteristics. For DUMAND, however, we are interested in photon collection rather than image formation. Furthermore there are well-recognized difficulties in measuring the attenuation length with short light-path instruments in very clear water: The attenuation length of blue-green light in very clear seawater is the order of 30 m, producing an attenuation of $(1-e^{-0.03})$, or 3% in 1 m pathlength. Experiments must be done skillfully to yield accurate values of attenuation length. For this reason short light path measurements are often made with red light whose intensity is reduced by 20% or more in reaching the detector. The attenuation length for 480 nm blue-green light is then calculated by using laboratory measurements of pure water attenuation at different wavelengths. Unfortunately the published ratios of red/blue-green attenuation coefficients differ by almost a factor of 2.

For these reasons measurements were made near the DUMAND site, using an uncollimated instrument with variable light+ path up to 84 m length.

Instrument

Basically, the instrument is a wide angle pulsed light source hung on a wire below a photodetector as shown schematically in Figure 1. The output of the photodetector is integrated, digitized, tone coded, as shown in Figure 2, and sent to shipboard for recording and monitoring. Observations are made at two or more source-detector distances to eliminate need for absolute calibration of source and detector.

The source is a voltage-regulated commercial photo-strobe (Sunpak 420) in a 13 cm dia aluminum pressure case. An RC solid state timer trigger the flash

*Permanent address, University of California, San Diego.

+We use the term "transmission distance β" to avoid confusion between these uncollimated observations and collimated beam observations that optical oceanographers designate by "attenuation length α".

Final Technical Report on Contract: N00014-79-C-0818

There were three parts to subject contract:

1. Design and construction of a novel instrument to measure the uncollimated attentuation length of blue-green light in seawater (H. Bradner):

   Measurements at approximately 1 km and 1.5 km depths, 27 km east of the center of the proposed DUMAND site off Keahole Point, Hawaii, gave an $\frac{1}{e}$ attentuation length of approximately 26 ± 1 meter at both depths. The work was reported the Proceedings of the 1980 International DUMAND Symposium.

2. Studies connected with adapting optical detector technology to the deep ocean environment (J. Learned):

   An instrument consisting of a string of 5 photomultipliers with very fast electronics has been designed and built, using funds from ONR, DOE, and the State of Hawaii. The instrument has been tested satisfactorily. Two weeks of muon intensity measurements are scheduled on the AGOR ship Desteiger, in February and March 1982.

3. Measurements of high frequency sound background deep in the ocean (V.C. Anderson & J. Presley):

   The instrument was designed to be attached to the "Deep tow" coaxial cable, and was intended to be used during cable tests at sea. The Deep-tow operation schedule permitted only two deployments of the sensitive high frequency acoustic detectors. Both measurements were too shallow for meaningful results. We hope to make deep measurements at the time of the above mentioned deployment in February and March 1982, at no additional cost to ONR.

every half minute. A 23 cm diameter opal glass on the front of a commercial photoflood reflector produces the intensity distribution in water shown in Figure 3.

The wire connecting source to detector is 1/8 inch diameter clean stainless steel. Optical path length of a measurement is set by choice of pre-prepared cable length.

The detector is housed in a 20 cm diameter aluminum pressure case with conical lucite window. Light entering through the window passes through a 480 nm wavelength, 10 nm bandwidth, interference filter. It is detected by an EG&G model HUV 4000-B silicon diode photovoltaic cell which has an incorporated operational amplifier.

The HUV-4000B is hermetically sealed for stability of components including a 200 MΩ feedback resistor in the op-amp. For measurements with 84 m light path the HUV 4000-B is used at full gain; for measurements with 7.86 m light path an external 401 KΩ is connected in parallel with the 200 MΩ internal resistor. Calibration procedures for this change in sensitivity are described in the Discussion section.

The output of the HUV 4000-B is integrated via an OP-07 ultra low offset op amp. The integrator output is reset to +4V every 4 sec. The millisecond duration light pulse produces an abrupt step toward zero in the integrated voltage. The non-zero dark output of the HUV 4000-B produces a slow drift in the integrated voltage, which is corrected for in calculating the pulse amplitude.

The integrated signal is digitized by a Burr Brown ADC 80, then put into 12 bit serial form, tone coded, and transmittted via 1/4" hydrographic wire to shipboard.

On board ship the signal is split for direct viewing on oscilloscope, tone code digital recording on magnetic tape cassette, and analog recording on strip chart. The digital tape is later read by computer for accurate data analysis.

Data analysis

Scattering of blue-green light in clear ocean water is sharply peaked forward, and has a coefficient in good geometry experiments only about 10% as large as the absorption coefficient. Therefore attenuation of point source monochromatic light can be considered exponential. The intensity from initial I_o after traveling short path S=7.87 m or long path L=84.00 m can be written as

$$I_S = \frac{I_o}{S^2} e^{-S/\beta} \; ; \; I_L = \frac{I_o}{L^2} e^{-L/\beta} \tag{1}$$

Combining, we get the 1/e transmission distance ,

$$\beta = \frac{L - S}{\ln \frac{S^2 I_S}{L^2 I_L}} = \frac{76.13}{\ln 0.00878 \; I_S/I_L} \; . \tag{2}$$

Note from equation (2) that the sensitivity of β to changes in I is

$$\frac{\delta\beta}{\beta} = \frac{\beta}{L - S}\,\frac{\delta I_L}{I_L} \tag{3}$$

and a similar expression, except for sign, for $\delta I_S/I_S$.
In our experiments β is approximately 25 m, so

$$\frac{\delta\beta}{\beta} \doteq \frac{1}{3}\,\frac{\delta I}{I} \tag{4}$$

Observations and Results

Measurements were made at two depths near the East edge of the Keahole site, using source-detector separations 7.87 m and 84.0 m length. Locations were 19°48'N; 156°24'W for the short cable and 19°50'N; 156°25'W for the long cable. Depths determined by length of cable were 1 km and 1.5 km. More accurate depths, determined by an acoustic pinger attached to the photodetector frame, are shown in Table II.

Observed values of transmitted light are summarized in Table 1. The last two columns show the calculated values of β for various data cuts, and the percent uncertainty of β based only on the pulse to pulse variation of recorded intensity.

As will be indicated in the Discussion, this pulse to pulse variation can be attributed to relative motion of source and detector, and it will always result in reduced recorded intensity. For this reason the data are separated into three groups: the average of the 3 highest received pulses, the average of the upper half of received pulses, and the average of all received pulses. The full distributions of received pulses are shown in Figure 4 and Figure 5. Note that the transmission distance differs by only ~5% at the two depths; therefore Table 1 also shows our data with all our observed values at the two depths combined.

Discussion

Sites of these observations are the island slope; visual and photographic observations during the search for RVWS showed that near-bottom water in this region was less clear than the central Keahole Basin (Ref., NOSC unpublished communication). The calculated value of β must be examined for a number of corrections and uncertainties. The most significant of these are tabulated and discussed below. δβ/β is the calculated 1σ value, where applicable. A positive value of δβ/β indicates that the true value of β is increased.

	δβ β
Size of source (Spreading is not $1/R^2$)	< +0.03%
Cable length (±2 mm for S; ±1 cm for L)	< ±0.02%
Cable twist(1)	-2, +2.2%
Source and detector tilt(2)	±1%
Pulse-to-pulse variation in source(3)	±0.7%
Detector gain calibration(4)	±0.2%
Worst case sum(5)	-4, +4.7%

Notes:

1) Twist in the 1/8" diameter cable connecting source to detector will move them out of optical alignment, thus reducing received light because of off-axis illumination and increased separation. The most severe effect is 5.5° misalignment for the 7.87 m wire when the source is twisted 180° away from detector. Figure 3 shows that the apparent source level for this case is reduced a factor of 0.995; the detector sensitivity is reduced by a factor of 0.975; and the inverse square correction is 0.990 for a total intensity reduction of 0.960. The effects for the 84 m wire are negligibly small.

Additional effects near 180° twist are the partial obscuring of the light beam by the 7.87 m wire, and a further obscuring of the light beam by a 4.7 cm O.D. shackle in the 84 m wire.

If all light striking the wire is lost from the detector, the intensity will be reduced by 3%. The shackle produces an additional 3% reduction. Combining all the above gives worst case intensity corrections of

$$\frac{\delta I_S}{I_S} = 6.5\% \,, \; \frac{\delta I_L}{I_L} = 6\% \; ; \text{ or } \frac{\delta\beta}{\beta} = -2, +2.2\%$$

2) Source and detector were balanced in calm sea water to better than 2° which can be seen from Figure 2 to give uncertainty of less than 1/2% in intensity, or less that 1/6% in $\delta\beta/\beta$.

Surface currents and winds at Keahole site caused the ship to drift at approximately 1 kt, while currents at 1 km depth were much smaller. Therefore the instrument was dragged through the water at a quasi-steady speed of about 1 kt, or 50 cm/sec. The wire connecting detector to source therefore hung in approximately a parabola, causing them to be optically misaligned (The figure is more like a uniformly loaded suspension bridge than a free-hanging catenary cable.) As shown in Figure 2, detector alignment is more critical than source alignment. In a 1 kt current the equilibrium source misalignment is calculated to be approximately 1° due to water drag; oscillations of 5 times this amplitude in the flowing water would still lead to a correction <2% in output signal, or 2/3% in $\delta\beta/\beta$ An upper limit of combined tilt effects is taken to be 1%.

The effect of current shear could be seen visually in the "wire angle" of the signal cable from the ship, and could be seen on the acoustic depth record which showed as much as 20 m/minute decrease in instrument depth for several minutes after the 1 km or 1.5 km cable was "payed out." Recorded depths vs times are shown in Table II.

All of the above rotations and misalignments will result in reduced received signals. However, since either the short or the long cable could suffer the reduction, the effect on β could be either an increase or a decrease in β.

3) The charging time between flashes is less than 10 sec, while flash rate is 2/minute.

At this repetition rate integrated light output at room temperature is independent of supply voltage between at least 4.5 and 6.5 volts, and is constant from pulse-to-pulse with standard deviation of 0.67%. In a test run of 33

flashes the maximum integrated output exceeded the average by less than 1.5%. Capacitance of the energy-storage capacitors decreases 4% when cooled from 24°C to 0°C, but this is unimportant since the aluminum capacitor case is held tightly against the aluminum pressure case, thus bringing its temperature essentially to surrounding sea water before light transmission measurements are made for either path length.

4) The ratio of detector gains used with the two cable lengths was determined in the laboratory. A two-step process, with a D.C. incandescent lamp was employed for maximum accuracy in the large gain ratio (428.0). The output of the HUV 4000-B at one light intensity was measured with a digital voltmeter for a reference 9 MΩ vs the 401 KΩ resistor used in the sea measurements; and the output at another light intensity was measured for the 9 MΩ vs the unshunted (viz 200 MΩ) condition. Standard deviation on repeated measurements was 0.05% for 9 MΩ vs 401 KΩ, and 0.2% for 9 MΩ vs 200 MΩ. The reduced accuracy in the latter case was caused by the increased amplifier drift at 200 MΩ.

The temperature coefficient of the HUV 4000-B with 200 MΩ internal resistor is claimed to be $\sim$0.01% per °C.

These errors cannot readily be combined statistically, so we add them and round off the result to give the "worst case sum of errors" of -4% +4.7%.

An alternative approach to error analysis is to consider the pulse to pulse variation in light recorded during the observations at sea. The data presented in Table I show standard deviation in good agreement with the detailed error analysis.

As an indicator of reliability we have also calculated β by using the highest values for I_S, and all the values for I_L. The resulting β is 24.12 m.

Conclusion

The best value of 1/e transmission distance at 1.5 km depth, calculated from the 3 highest pulses, is $\beta \doteq 25.9$ m. The value calculated from all 1.5 km data is 25.3 m. Probable errors can not be fully described statistically, but error analysis made by three different methods all lead to comparable estimates of $\delta\beta \doteq 1$ m. The reduced transmission at 1 km depth, and the difference between our observed value of $\beta \doteq 25$ m vs. Zaneveld's $1/a \doteq 40$ m, (Ref. Ron Zaneveld in these Proceedings) lends emphasis to the need for side by side measurements by both instruments in the center of Keahole site.

This work was supported by ONR grants to Scripps Institution of Oceanography and the University Hawaii as well as funds from Hawaii Institute of Geophysics.

Table I

~~TRANSMISSOMETER DATA~~

DEPTH	SAMPLES	I_S	σ/β (%)	I_L	σ/β (%)	$\hat{\beta}$ (meters)	σ/β (%)
1 km*	Highest 3	2061		343.7		24.4	
	Upper half	2019	2.3	337	2	24.4	1
	All	1910	6.7	305.9	12	24.1	4.6
1.5 km*	Highest 3	2032		402.7		25.9	
	Upper half	1985	2.5	381.1	5	25.6	1.9
	All	1908	5.2	352.5	10	25.3	3.8
Combined	Highest 3	2065		402.7		25.7	
	Upper half	2003	2.6	360.2	7	25.1	2.6
	All	1910	6.1	330.5	13	24.7	4.8

*Nominal depth were 1 km and 1.5 km. See text for details.

TABLE II

INSTRUMENT DEPTH, DETERMINED BY ACOUSTIC PINGER

DATE-TIME		WIRE	CABLE PAYED OUT	INSTRUMENT DEPTH
7/9/80	2020Z	7.87 m	1.0 km	789 m
	2040			758
	2048		1.5*	1211
	2102			1116
7/10/80	1058Z	84 m	1.0 km	870 m
	1106			872
	1113		1.5	1339
	1125			1290

*Note: Pinger indicates that 1.5 km was not payed out.

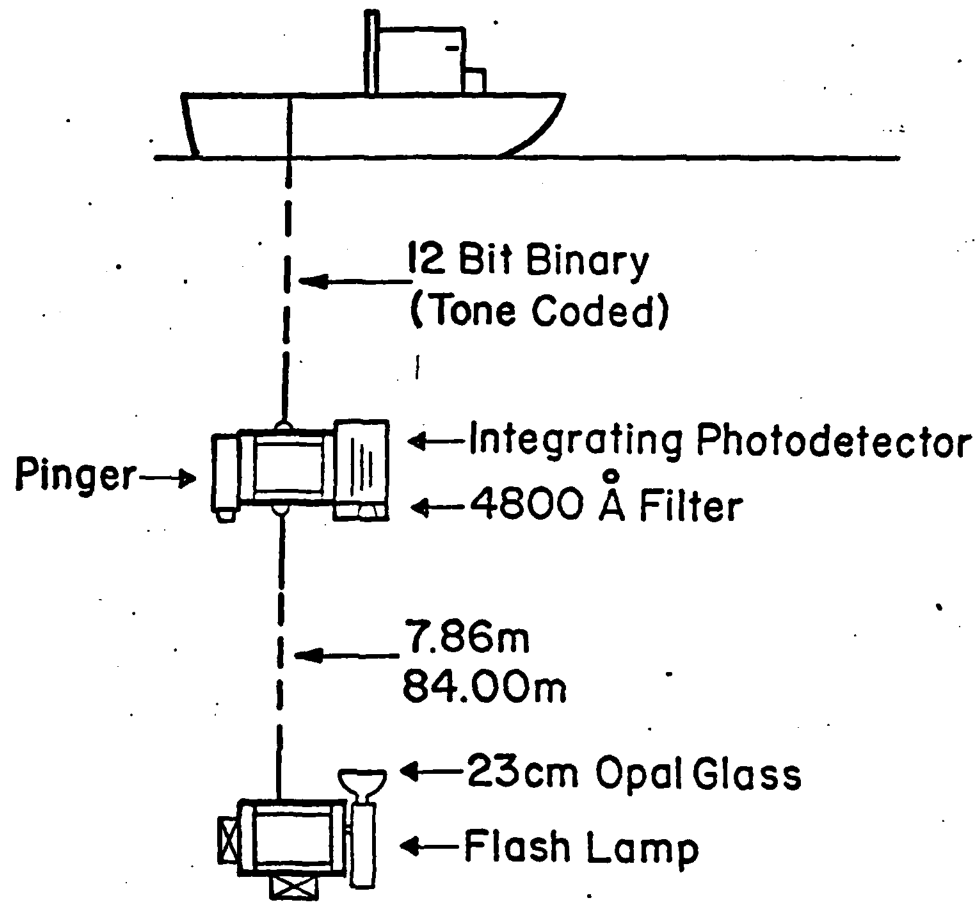

FIG. I
SYSTEMATIC SCHEMATIC

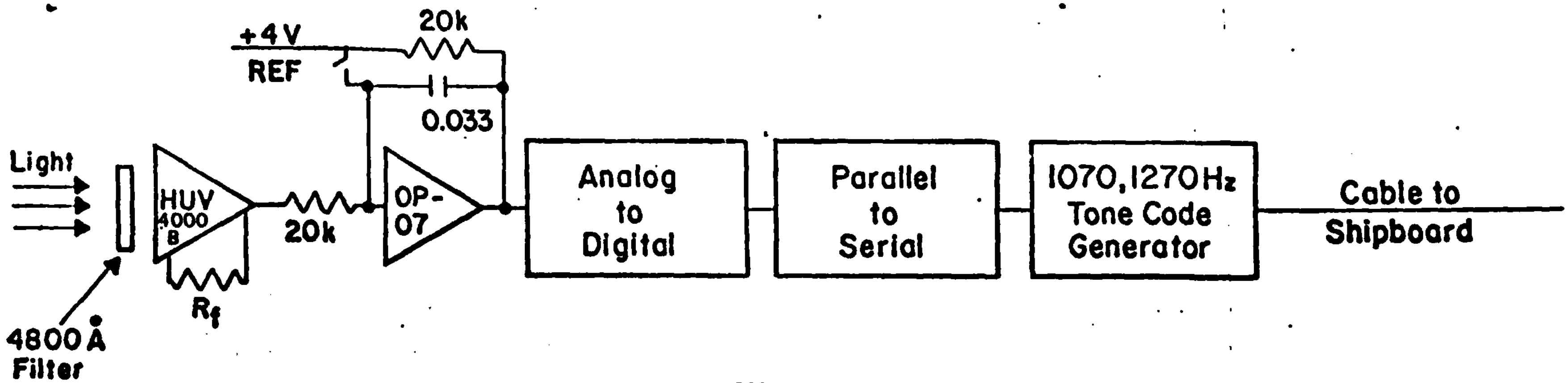

FIG. 2
PHOTODETECTOR SCHEMATIC

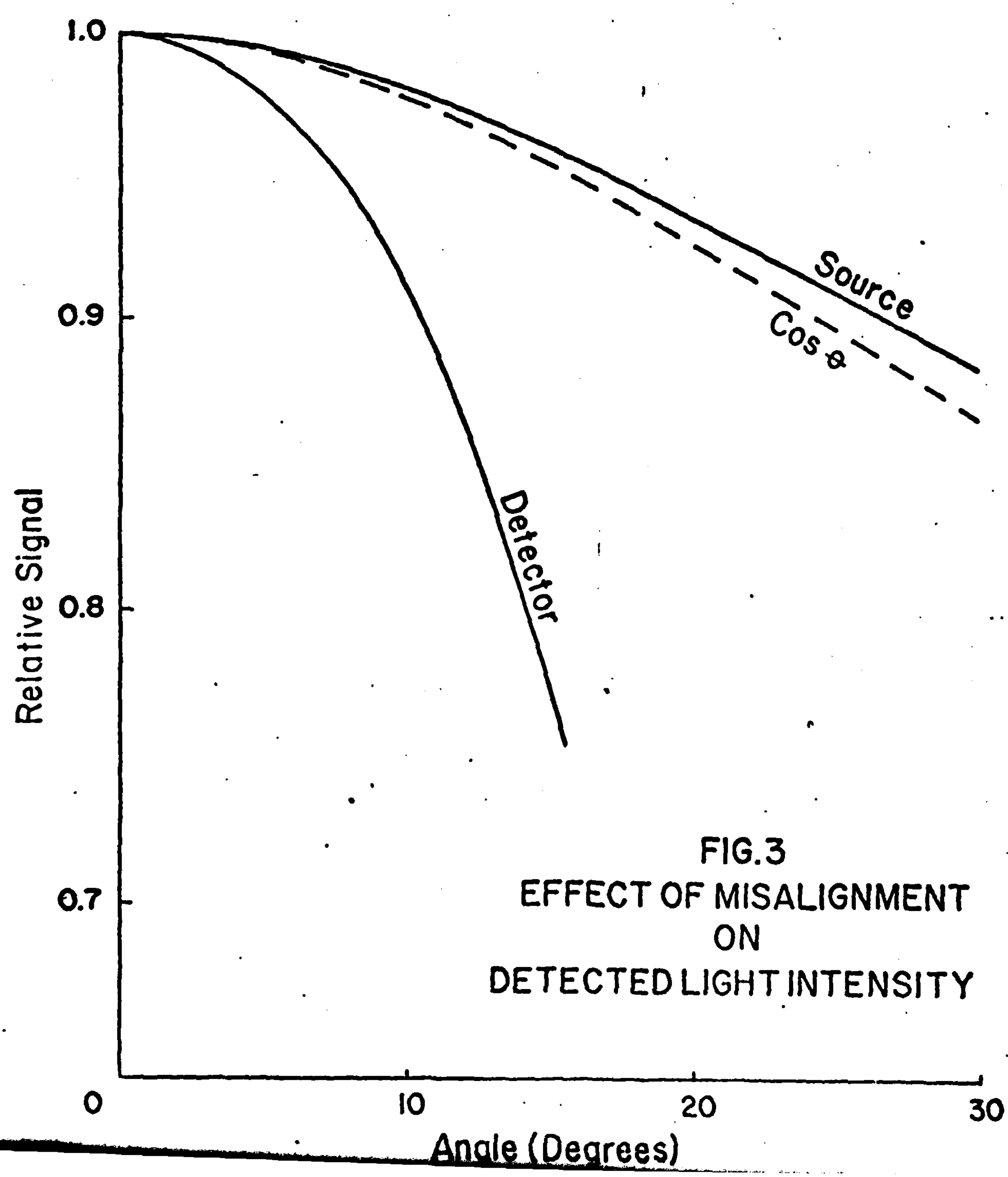

FIG.3
EFFECT OF MISALIGNMENT
ON
DETECTED LIGHT INTENSITY

FIG. 4

RECEIVED INTENSITY
SHORT CABLE

x 1 KM DEPTH
• 1.5 KM DEPTH

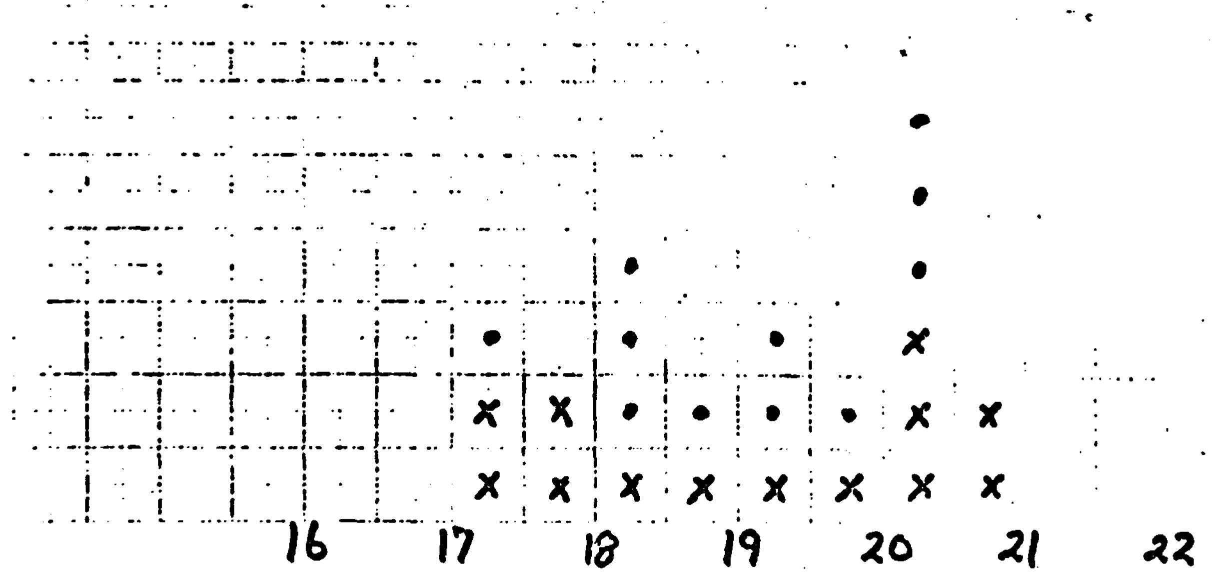

FIG. 5

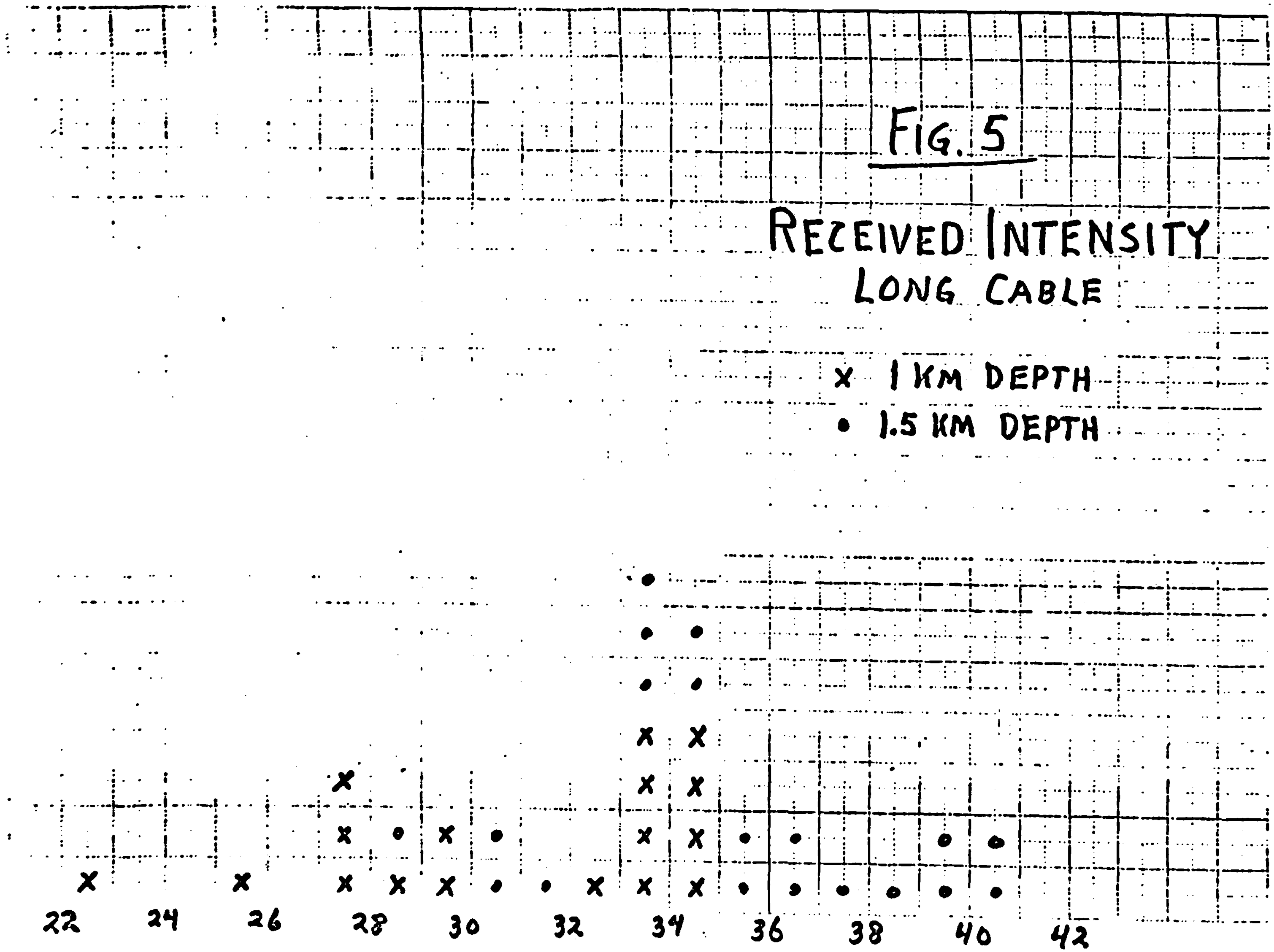
RECEIVED INTENSITY
LONG CABLE
x 1 KM DEPTH
• 1.5 KM DEPTH
22
24
26
28
30
32
34
36
38
40
42

DA

FILM